Reprinted from:
ADVANCES IN HEAT TRANSFER, VOL. 13

ACADEMIC PRESS, INC.
NEW YORK SAN FRANCISCO LONDON

Viscous Dissipation in Shear Flows of Molten Polymers

HORST HENNING WINTER

Institut für Kunststofftechnologie, Universität Stuttgart, Stuttgart, West Germany

I. Introduction

Polymer processing and applied polymer rheology occur at relatively high temperatures and often at high temperature gradients. In molten polymers, large stresses are required to maintain the flow and, additionally to convective and conductive heat transfer, temperatures essentially depend on viscous dissipation, i.e., on conversion of mechanical energy into heat. Velocity and temperature fields influence each other: the temperatures influence the flow through the temperature-dependent rheological properties, and the velocities influence the temperatures through convection, through dissipation, and through anisotropical effects (which are investigated very little) on the thermal properties.

Research in rheology and in thermodynamics related to heat transfer problems is mostly done separately, by rheologists on molten polymers or polymer solutions at constant temperature, and by thermodynamicists on polymers at rest. The difficult task of combining the two areas is left to the polymer engineers (see for instance [1–4]). A number of assumptions have to be introduced into the heat transfer analysis before applied problems can be solved.

The different flow problems involving heat transfer and viscous dissipation can be classified in groups as shown in Table I. Each of the groups is characterized by different rheological phenomena, and one has to choose very different rheological constitutive equations to describe them. The two main groups are *channel flow* (including flow geometries with partly solid and partly free boundary) and *free surface flow* (with no solid boundary). In polymer processing, channel flow of molten polymers occurs in a large variety of flow geometries. The polymer is forced through a channel by a pressure gradient (flow in an extruder die, for instance), or it is dragged along by a moving wall (rotating screw in a stationary cylinder, for instance). Very often both types of flow are superimposed on each other. Free surface flow for example occurs in film blowing or fiber spinning.

TABLE I

CLASSIFICATION OF HEAT TRANSFER AND VISCOUS DISSIPATION IN MOLTEN POLYMERS

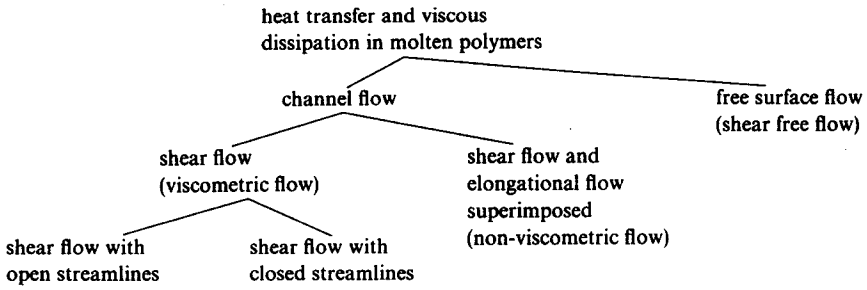

For rheological reasons, channel flow problems are subdivided into *shear flow* (also called viscometric flow) and *nonviscometric* flow. The separation of the shear flow problems into one group with open stream lines and one with closed stream lines has to be made since their thermal development is different.

Throughout the first section, the heat transfer problem will be considered in general, i.e., the relevant equations are listed in a general form and the properties are described. The *rheological* properties of the molten polymers have to be formulated differently according to the various flow types since

the length of the following sections is supposed to reflect the degree of understanding of the respective flow and heat transfer problems.

In Section II, heat transfer in shear flow will be analyzed. A large emphasis will be laid on replacing the commonly used idealized boundary conditions, i.e., constant wall temperature or constant wall heat flux (with the limiting case of the adiabatic wall), by more general conditions. In practical applications, the idealized conditions will rarely occur; actually it is difficult to achieve them even in especially designed model experiments. To make the analysis applicable, heat transfer in a flowing polymer should not be studied separately inside the fluid, but together with the surrounding wall.

In this analysis the heat transfer at the wall is described by an outer temperature difference (temperature of the surroundings minus temperature at the boundary) and the *Biot number*, which otherwise has been used successfully for describing the boundary conditions for temperature calculations in solids. The Biot number is appropriate for describing boundary conditions between isothermal and adiabatical, as they occur in real processes. Additionally, the thermal capacity of the walls is included in the analysis by introducing the *capacitance parameter C*.

Heat transfer in viscometric flow has been studied quite extensively in the literature, and at the present state it seems to be necessary to show the many common aspects of the different studies. Thus, as the main goal of this study a unifying concept will be developed. This concept makes it possible to *comprise the most important shear flow cases into a single one*, which can be solved with *one* numerical program.

For Section III on nonviscometric flow in channels and flow with free boundaries, the description will not go much further than stating the problem, showing the present methods of solution, and listing references. Since nearly all of the results in this report are on shear flow, the title is taken to be "in shear flows" even if the problem is stated in a general form and Section III is on nonviscometric flows.

Heat transfer in non-Newtonian fluids at *negligible* viscous dissipation is not included in this report (see instead [5–7]), although it can be treated as a limiting case of the corresponding flow with viscous dissipation.

A. SYSTEM OF EQUATIONS

The problems are governed by the equations describing the conservation of mass

$$\partial\rho/\partial t + \nabla \cdot (\rho \mathbf{v}) = 0 \tag{1.1}$$

and the conservation of energy

$$\rho\, De/Dt = \nabla \cdot (k\, \nabla T) + \boldsymbol{\sigma} : \nabla \mathbf{v}, \tag{1.2}$$

by the stress equation of motion

$$\rho\, D\mathbf{v}/Dt = \nabla \cdot \boldsymbol{\sigma} + \rho\mathbf{g}, \tag{1.3}$$

and by the constitutive equation which will be described below, together with the appropriate flow geometries. The three equations above are derived and tabulated in textbooks (see for instance [8]) for different coordinate systems.

∂/∂ denotes the partial and D/D the substantial derivative; ∇ is the "nabla" operator. Density ρ and thermal conductivity k are properties of the fluid. Velocity $\mathbf{v}$, internal energy e, temperature T, time t, and stress $\boldsymbol{\sigma}$ are the variables. The stress $\boldsymbol{\sigma}$ is defined in such a way that the force on the positive side of a surface element of unit area and normal vector $\mathbf{n}$ is $\mathbf{n} \cdot \boldsymbol{\sigma}$.

The equation of energy says that the rate of gain of internal energy per unit volume ($\rho\, De/Dt$) is equal to the rate of internal energy input by conduction per unit volume $\nabla \cdot (k\, \nabla T)$ plus the rate of work by the stress on the volume element $\boldsymbol{\sigma}:\nabla\mathbf{v}$, which is being partly stored and partly dissipated during the flow. For heat transfer studies, the internal energy has to be defined in terms of the fluid temperature and the strain and stress variables.

Incompressible fluid: In rheology the fluid is usually supposed to be incompressible (even when properties such as the viscosity are allowed to depend on pressure). The flow geometry, the temperature, and the rheological properties of the fluid determine the stress completely, *except for an arbitrary added isotropic pressure* [9]. Therefore, the stress is commonly separated into an arbitrary pressure p and the extra stress $\boldsymbol{\tau}$, which is defined in the rheological constitutive equation, viz.

$$\boldsymbol{\sigma} = -p\boldsymbol{\delta} + \boldsymbol{\tau}. \tag{1.4}$$

$\boldsymbol{\delta}$ denotes the unit tensor.

In some flow problems, it is convenient to define the isotropic pressure p to be equal to one of the normal stress components in a certain coordinate system ($p = -\sigma_{11}$, $p = -\sigma_{22}$, or $p = -\sigma_{33}$), while in other flow problems it might be preferable to define $p = -(\text{trace}\ \boldsymbol{\sigma})/3$.

For an "incompressible" fluid, the change in internal energy and the work of the stress per unit time are determined by

$$\begin{aligned} \rho\, De/Dt &= c\rho\, DT/Dt, \\ \boldsymbol{\sigma}:\nabla\mathbf{v} &= -p\, \nabla \cdot \mathbf{v} + \boldsymbol{\tau}:\nabla\mathbf{v}, \end{aligned} \tag{1.5}$$

and Eq. (1.2) becomes

$$c\rho\, DT/Dt = \nabla \cdot (k\, \nabla T) + \boldsymbol{\tau}:\nabla\mathbf{v}. \tag{1.6}$$

The specific heat capacity c is defined as the thermal energy needed per unit mass and Kelvin degree for changing the temperature of a material. Since the density is taken to be constant, c has to be measured at constant

density. If the fluid were really incompressible, the specific heat should be the same for measurements at constant density (c_v) or at constant pressure (c_p). From thermodynamic data at rest (Eq. (1.11)), however, one finds that c_p and c_v of polymer melts differ by about 10%.

Compressible fluid: There are difficulties in relating strain and stress in deforming materials that are slightly compressible. One commonly assumes that the deformation can be separated into two parts: a deformation at constant density and the volume change [10]. Neglecting the influence on each other, the deformation at constant density is described by the constitutive equation, and the density of the flowing polymer is determined from equilibrium data $\rho(T, p)$ measured on the fluid at rest (taking $p = -(\text{trace } \boldsymbol{\sigma})/3$).

There also seem to be difficulties in defining the internal energy e of a compressible flowing fluid: one assumes that e can be described in terms of p and ρ only, independently of the other stress and strain variables (see for instance [8]):

$$e = e(p, \rho).$$

Applying this relation to the flowing polymer melt, the substantial derivative of the internal energy then becomes

$$\rho \frac{De}{Dt} = -p \nabla \cdot \mathbf{v} + \epsilon T \frac{Dp}{Dt} + \rho c_p \frac{DT}{Dt} \tag{1.7}$$

with $\epsilon = -\rho^{-1}(\partial\rho/\partial T)_p$, the coefficient of thermal expansion. ϵ and c_p are evaluated from rest data at temperature T and the "pressure" $p = -(\text{trace } \boldsymbol{\sigma})/3$. The equation of energy takes the form usually shown in the literature [11]:

$$\rho c_p \frac{DT}{Dt} = \nabla \cdot (k \nabla T) + \epsilon T \frac{Dp}{Dt} + \boldsymbol{\tau} : \nabla \mathbf{v}. \tag{1.8}$$

From this equation, calculated temperature fields in channel flow (see Fig. 13, p. 244) show large temperature decreases due to cooling by expansion. The assumptions made above (concerning the density changes and the internal energy) are rather severe, and further experimental studies are needed to investigate their validity.

B. THERMAL PROPERTIES

The properties in the analysis are the density ρ, the specific heat c, and the thermal conductivity k; the thermal diffusivity is defined as $a = k/\rho c$. Rheological properties are defined separately in the constitutive equation.

In a stationary fluid, the density $\rho(p, T)$ is a function of pressure and temperature. It can be described by the equation of Spencer and Gilmore

TABLE II

MATERIAL CONSTANTS OF EQ. (1.9) MEASURED BY SPENCER AND GILMORE [12]

polymer	b^* [10^{-3} m^3/kg]	p^* [N/m^2]	W [10^{-3} kg/g-mole]
l.d.PE	0.875	3.275×10^8	28
PS	0.822	1.863×10^8	104
PMMA	0.734	2.157×10^8	100
CAB	0.688	2.844×10^8	54

[12]:

$$(1/\rho - b^*)(p + p^*) = RT/W, \tag{1.9}$$

where b^*, p^*, and W are material constants. Their values are tabulated (Table II) for some examples of the most widely used polymers; $R = 8.314$ [J/K g-mole] is the gas law constant.

From Eq. (1.9) one can evaluate the term ϵT of the equation of energy

$$\epsilon T = 1 - \rho b^*; \tag{1.10}$$

since b^* is always smaller than ρ^{-1}, the *dimensionless product* ϵT *adopts positive values smaller than unity.*

The density generally is measured on the polymer at rest and in thermodynamic equilibrium. Dynamic measurements by Matsuoka and Maxwell [13], however, show a very delayed response of polyolefines to sudden pressure changes. Thus, the use of equilibrium density data restricts the analysis to flows of slowly changing pressures. The reaction to temperature changes is similarly delayed [14]. Additionally the flow might influence the density.

The specific heat commonly is measured at constant pressure. Using the equation proposed by Spencer and Gilmore, Eq. (1.9), one can determine the specific heat at constant density c_v from specific heat data at constant pressure c_p [4]:

$$c_v = c_p - R/W. \tag{1.11}$$

The thermal conductivity k and the specific heat capacity c_p are slowly varying functions with temperature and they also depend on pressure. In flowing polymers the thermal conductivity possibly varies with direction. For most polymers the temperature dependence can be expressed in a linear form

$$\begin{aligned} k &= \bar{k}(1 + a_k(T - T_0)), \\ c_p &= \bar{c}_p(1 + a_c(T - T_0)). \end{aligned} \tag{1.12}$$

$\bar{k}$ and $\bar{c}_p$ are values at some reference condition (temperature T_0), while a_k and a_c are the temperature coefficients, which might be positive or negative

TABLE III

THERMAL CONDUCTIVITY AND SPECIFIC HEAT CAPACITY OF SOME MOLTEN POLYMERS AT TEMPERATURES T_0 (see [15–23])

Polymer	T_0 [°C]	c_p [10^3 Nm/kg K]	k [N/K s]
l.d.PE	150	2.57	0.241
h.d.PE	150	2.65	0.255
PP	180	2.80	—
PVC	100	1.53	0.166
PS	150	2.04	0.167
PMMA	150	—	0.195

depending on the polymer in question and on the temperature range. Table III shows some values of k and c_p. More detailed data on the properties can be found in references [15–23], for instance.

C. RHEOLOGICAL CONSTITUTIVE EQUATION

For a large number of fluids, which can be regarded as incompressible, the stress can be described by the Stokes equation

$$\sigma = -p\delta + \eta\dot{\gamma}, \tag{1.13}$$

the simplest tensor generalization of Newton's law of viscosity. Here p is the isotropic pressure, and $\dot{\gamma} = (\nabla v) + (\nabla v)^+$ is the rate of strain tensor; the viscosity η depends on temperature and on pressure, but not on the time t or on any kinematic quantities such as $\dot{\gamma}$. Fluids that show this behavior are called *Newtonian.*

The Stokes equation has been generalized by taking the viscosity $\eta(\dot{\gamma})$ to be a function of the second invariant of the rate of strain tensor [24]:

$$\sigma = -p\,\delta + \eta(\dot{\gamma})\dot{\gamma}; \qquad \dot{\gamma} = (\tfrac{1}{2}\dot{\gamma}:\dot{\gamma})^{1/2}. \tag{1.14}$$

This equation defines the "generalized Newtonian fluid." It has been applied quite successfully to molten polymers in *steady shear flow* for calculating the *shear component* of the stress tensor in an appropriate coordinate system; however, the *normal stress components* calculated from this equation are known to be unrealistic for molten polymers. In general, the equation might be misleading in its tensor form because it does not allow one to calculate meaningful stress components in arbitrary coordinate systems. The appropriate statement of the rheological equation for molten polymers in steady shear flow is given by Criminale *et al.* [25]; their equation will be applied in Section II.

The rheological properties of elastic fluids (such as molten polymers) at any given position depend on the strain and temperature history of the fluid elements when they arrive at that position, independently of the history of neighboring particles. Translational and rotational movements do not influence the stress [9].

Depending on the type of flow, the rheological behavior of molten polymers is more or less different from the behavior of Newtonian fluids. Up to now there exists no general constitutive equation to describe all the phenomena known for a given polymer melt. Additionally, the temperature effects on the rheological properties have not been studied at all or only at different levels of homogeneous temperatures. The constitutive equations used will be stated in the beginning of Sections II and III.

II. Shear Flow (Viscometric Flow)

In shear flow at constant density, material surfaces move "rigidly" (i.e., without stretching) across each other. These surfaces are called *shear surfaces* [26]. Pipe flow, which is an example of shear flow, sometimes is called telescopic flow since its rigidly moving surfaces are concentric cylinders. In Fig. 1 the deformation of particle P_0 at the origin is described by the relative motion of neighboring planes. On the left (Fig. 1a) an orthonormal coordinate system is chosen, such that

x_1 = direction of shear,

x_2 = direction of velocity gradient,

x_3 = neutral direction.

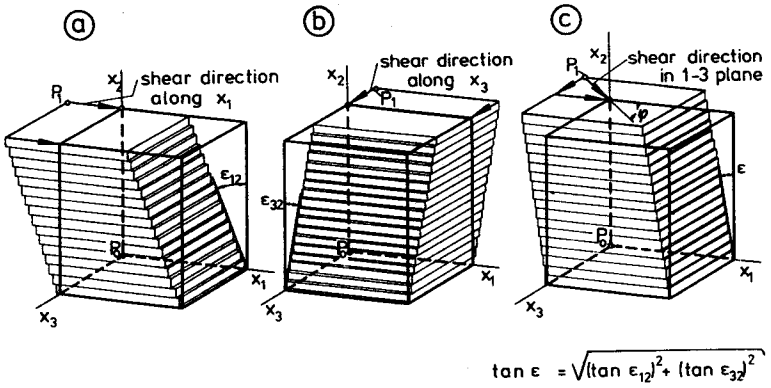

FIG. 1. Unidirectional shear flow in cartesian coordinates. Shear flow in the 1-3 plane as superposition of shear flow along x_1 and along x_3.

The *direction of shear* (or shear direction) and related quantities are defined following [26]: an orthonormal coordinate system is chosen to have its x_1 axis and its x_3 axis in a shear surface (see Fig. 1). The x_2 axis is perpendicular to the shear surface; it projects point P_0 onto neighboring shear surfaces. During shear flow, shear surfaces move past each other, and the normal projection of P_0 draws a line on neighboring shear surfaces. This line is called the *shear line.* (Note: In the examples of Fig. 1, the shear surfaces are planes, and the shear lines are straight.) The tangent to the shear line at time t is defined to be the *shear direction* at time t, and the angle of the shear line with the x_1 coordinate is the *shear angle* φ; if the direction of shear remains constant with time, the flow is called *unidirectional.* For most applications, the direction of shear is identical with the direction of flow; an exception is the othogonal rheometer [26, p. 76], for instance.

The shear rate, the extra stress, and the temperature are supposed to be uniform in the direction of shear, but they may change perpendicularly to the direction of shear (even within shear surfaces). If one allows for shear in the 3 direction (Fig. 1b) additionally to the shear in the 1 direction, the shear direction is in the 1-3 plane (Fig. 1c); for some steady shear flow geometries (as in helical flow), it is convenient to choose a global coordinate system with the velocity vector in the 1-3 plane and the velocity gradient normal to the 1-3 plane. The matrix of the rate of strain tensor becomes

$$[\dot{\gamma}] = \begin{bmatrix} 0 & \dot{\gamma}_{12} & 0 \\ \dot{\gamma}_{12} & 0 & \dot{\gamma}_{23} \\ 0 & \dot{\gamma}_{23} & 0 \end{bmatrix}, \tag{2.1}$$

and the second invariant of the rate of strain tensor defines the shear rate:

$$\dot{\gamma} = (\dot{\gamma}_{12}^2 + \dot{\gamma}_{23}^2)^{1/2}. \tag{2.2}$$

In unidirectional shear flow at constant temperature T_0, constant pressure p_0, and constant volume, the stress is given by the shear rate $\dot{\gamma}(t)$ and the three shear-rate-dependent viscometric functions [25, 26]:

viscosity $\eta(\dot{\gamma}^t_{-\infty}, T_0, p_0)$,
first normal stress coefficient $\psi_1(\dot{\gamma}^t_{-\infty}, T_0, p_0)$,
second normal stress coefficient $\psi_2(\dot{\gamma}^t_{-\infty}, T_0, p_0)$.

Here $\dot{\gamma}^t_{-\infty}$ symbolizes the "history of shear rates" to which the medium was submitted up to the present time t.

Up to now, there do not seem to exist heat transfer studies on shear flow in general; however for *steady* shear flow, the publications are numerous. In Section II.C.3 an example of heat transfer in unsteady unidirectional shear flow will be shown.

Steady Shear Flow and Shear Viscosity

For unsteady shear flow the shear direction and/or the value of the shear rate change with time; the shear surfaces, however, are maintained. If the shear direction and the shear rate are kept constant over some time (φ = const; $\dot{\gamma}$ = const), the shear stress approaches a constant value, i.e., the viscosity adopts a constant value:

$$\eta(\dot{\gamma}, T_0, p_0) = \lim_{t \to \infty} \eta(\dot{\gamma}'_{-\infty}, T_0, p_0), \tag{2.3}$$

called the *viscosity*, the *shear viscosity*, or the *apparent viscosity*. The flow becomes *steady (unidirectional) shear flow*. The index on T_0 and p_0 indicates that the viscosity is *defined at constant temperature and pressure.*

The elastic properties of the fluid are represented in steady shear flow by the two viscometric functions ψ_1, ψ_2. These functions, however, do not have any influence on heat transfer and viscous dissipation; this will be shown in the following.

The only two terms in the system of equations (Eqs. (1.1)–(1.3)) that contain the stress are $\boldsymbol{\sigma}:\nabla\mathbf{v}$ and $\nabla \cdot \boldsymbol{\sigma}$. The rate of work by the stress $\boldsymbol{\sigma}:\nabla\mathbf{v}$, which *in steady shear flow is dissipated completely*, sometimes is called the dissipation function. Taking the coordinate system of the shear flow, one can evaluate the two terms [8, p. 738]; $\boldsymbol{\sigma}:\nabla\mathbf{v}$ is a scalar

$$\boldsymbol{\sigma}:\nabla\mathbf{v} = \tau_{12}\dot{\gamma}_{12} + \tau_{23}\dot{\gamma}_{23}, \tag{2.4}$$

and $\nabla \cdot \boldsymbol{\sigma}$ is a vector with the three components

$$\begin{aligned}
[\nabla \cdot \boldsymbol{\sigma}]_1 &= \frac{\partial}{\partial x_1}(-p + \tau_{11}) + \frac{\partial}{\partial x_2}\tau_{12} + \frac{\partial}{\partial x_3}\tau_{13}, \\
[\nabla \cdot \boldsymbol{\sigma}]_2 &= \frac{\partial}{\partial x_1}\tau_{12} + \frac{\partial}{\partial x_2}(-p + \tau_{22}) + \frac{\partial}{\partial x_3}\tau_{23}, \\
[\nabla \cdot \boldsymbol{\sigma}]_3 &= \frac{\partial}{\partial x_1}\tau_{13} + \frac{\partial}{\partial x_2}\tau_{23} + \frac{\partial}{\partial x_3}(-p + \tau_{33}).
\end{aligned} \tag{2.5}$$

The stress $\boldsymbol{\sigma}$ has been decomposed into p and τ as shown in Eq. (1.4). If x_1 is the shear direction (Fig. 1a), the 1 component of $\nabla \cdot \boldsymbol{\sigma}$ is used for calculating the velocity and the pressure gradient; due to the symmetry of the flow ($\partial\tau/\partial x_1 = 0$); and since $\tau_{13} = 0$, the 1 component reduces to

$$[\nabla \cdot \boldsymbol{\sigma}]_1 = -\frac{\partial p}{\partial x_1} + \frac{\partial \tau_{12}}{\partial x_2}. \tag{2.6}$$

For a shear direction in the 1-3 plane (Fig. 1c), the 1 and the 3 components are used for calculating the velocity and the pressure gradient; since $\partial\tau/\partial x_1 = 0$

and $\partial\tau/\partial x_3 = 0$, they reduce to

$$[\nabla \cdot \boldsymbol{\sigma}]_1 = -\frac{\partial p}{\partial x_1} + \frac{\partial \tau_{12}}{\partial x_2}, \qquad [\nabla \cdot \boldsymbol{\sigma}]_3 = -\frac{\partial p}{\partial x_3} + \frac{\partial \tau_{23}}{\partial x_2}. \tag{2.7}$$

For calculating the velocity, the pressure gradient, and the rate of work by the stress, one finds from Eqs. (2.4), (2.6), (2.7) that one needs only the shear components τ_{12}, τ_{23} of the stress matrix

$$\tau_{12} = \eta(\dot{\gamma}, T) \cdot \dot{\gamma}_{12}, \qquad \tau_{23} = \eta(\dot{\gamma}, T) \cdot \dot{\gamma}_{23}. \tag{2.8}$$

The shear component $\tau_{13} = \sin 2\varphi(\psi_1 + \psi_2)\dot{\gamma}^2/2$ and the normal stress components do not contribute to the analysis. *The viscosity η is the only rheological property needed* for solving heat transfer problems in unidirectional steady shear flow. Thus the heat transfer analysis of Section II is *not restricted to purely viscous fluids*, even if the normal stresses are not mentioned further.

The pressure and the normal stresses can separately be determined from the pressure gradient, the 2 component of the stress equation of motion (which contains $[\nabla \cdot \boldsymbol{\sigma}]_2$), and the appropriate boundary conditions.

Some typical curves of viscosities referring to different temperatures are shown in Fig. 2 [27]. At low shear rates ($\dot{\gamma} < 10\ s^{-1}$) one measures the viscosity in Couette or in cone and plate rheometers, and at high shear rates ($\dot{\gamma} > 1\ s^{-1}$) one uses a capillary or slit viscometer; the temperature in the test section is kept as uniform as possible.

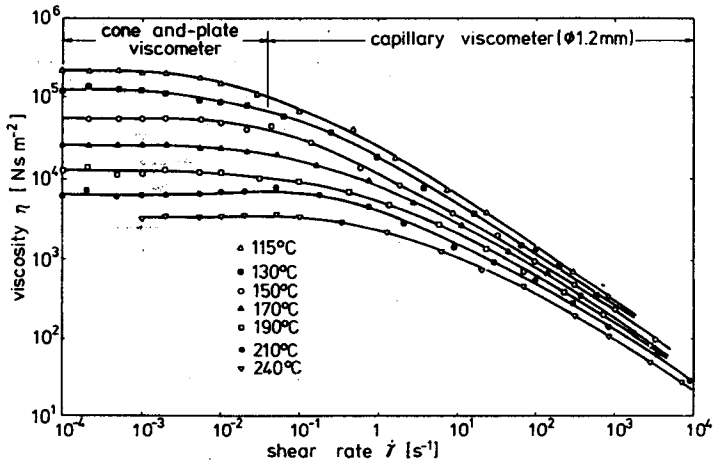

FIG. 2. Typical viscosity curve of molten polymer (low density polyethylene) measured by Meissner [27].

The pressure and temperature dependence of the viscosity usually is described by the corresponding coefficients

$$\text{pressure coefficient} \qquad \alpha = \frac{1}{\eta}\left(\frac{\partial \eta}{\partial p}\right)_{\dot{\gamma},T}, \tag{2.9}$$

$$\text{temperature coefficient} \qquad \beta = -\frac{1}{\eta}\left(\frac{\partial \eta}{\partial T}\right)_{\dot{\gamma},p}. \tag{2.10}$$

(Note: Some authors define the temperature coefficient β at constant shear stress instead of at constant shear rate.) In the expression for the viscosity, the variables are separated. The pressure dependence is described by an exponential function. For incorporating the temperature dependence one may take just an exponential function

$$\eta(\dot{\gamma}, T, p) = f(\dot{\gamma}, p)\exp(-\beta T) \tag{2.11}$$

or use an Arrhenius type expression

$$\eta(\dot{\gamma}, T, p) = f(\dot{\gamma}, p)\exp(E/RT) \tag{2.12}$$

whose "activation energy" E has been reported to be a material constant over wide temperature ranges [28, 29]. The temperature coefficient of the viscosity at temperatures around T_0 can then be determined as (if one expands (E/RT) around T_0)

$$\beta(T_0) = E/RT_0^2 \tag{2.13}$$

i.e., for constant E, the temperature coefficient is proportional T^{-2}. The temperature dependence of β normally is neglected in analytical studies, which is acceptable if the deviations ΔT from the temperature level T_0 are not too large. The relative difference of the two expressions, Eqs. (2.11) and (2.12), is

$$(\Delta\eta)_{\text{rel}} = \frac{\exp\left(\frac{E}{R}\left(\frac{1}{T} - \frac{1}{T_0}\right)\right) - \exp(-\beta(T - T_0))}{\exp\left(\frac{E}{R}\left(\frac{1}{T} - \frac{1}{T_0}\right)\right)}.$$

$$= 1 - \exp[-\beta(\Delta T)^2/(T_0 + \Delta T)]; \tag{2.14}$$

as an example $\Delta T = 10\,\text{K}$, $\beta = 10^{-2}\,\text{K}^{-1}$, $T_0 = 400\,\text{K}$ gives a relative difference of less than 0.25%.

At very low shear rates ($\dot{\gamma} < 10^{-1}$–10^{-3} depending on temperature, polymer, molecular weight distribution) the viscosity adopts a value inde-

pendent of shear rate, the zero viscosity $\eta_0(T, p)$ (see Fig. 2). At medium and high shear rates ($\dot{\gamma} > 10$), as they occur in polymer processing, the viscosity curve $\eta(\dot{\gamma})$ is nearly a straight line in the log–log plot. Ranges of the curve can be approximated by a power law [30] which will be formulated as

$$\frac{\eta}{\bar{\eta}} = \left(\frac{\dot{\gamma}}{\bar{\dot{\gamma}}}\right)^{(1/m)-1} \exp[\alpha(p - p_0) - \beta(T - T_0)]. \tag{2.15}$$

The power law exponent is different for different ranges of $\dot{\gamma}$, T, p; for molten polymers, the value of m is between 2 and 5. In Eq. (2.15), $\bar{\eta} = \eta(\bar{\dot{\gamma}}, p_0, T_0)$ is a reference viscosity within the power law region, i.e., η at the reference shear rate $\bar{\dot{\gamma}}$, at the reference pressure p_0, and at the reference temperature T_0. In the literature the power law model has been used very widely because its form allows direct integration of the equation of motion for several flow geometries to be carried out.

There are very few data on α and β available; however, α_0 and β_0 values of the zero viscosity η_0 have been published for several molten polymers. Thus, a relation will be derived in the following between α and α_0 and between β and β_0. The viscosity curves measured at different levels of T and p can be condensed to a single one, the so-called *master curve* [31, 32]

$$\eta(\dot{\gamma}, T, p)/\eta_0(T, p) = f(\dot{\gamma} \cdot \eta_0(T, p)). \tag{2.16}$$

In the transformation process, the viscosity curves are moved in the log–log plot in the direction of $-45°$; the shape of each curve remains the same. Therefore, the shape of the master curve is identical with the shape of the other viscosity curves. At larger values $\eta_0\dot{\gamma}$ ($>10^4$ N m^{-2}), ranges of the master curve can be fitted again by the power law shown above

$$\eta(\dot{\gamma}, T, p)/\eta_0(T, p) = K(\dot{\gamma}\eta_0)^{(1/m)-1}, \tag{2.17}$$

and the viscosity becomes

$$\eta(\dot{\gamma}, T, p) = K\eta_0^{1/m}\dot{\gamma}^{(1/m)-1}. \tag{2.18}$$

K is a "material constant" whose dimension depends on the value of the power law exponent m; K will be replaced by introducing the reference viscosity $\bar{\eta}$ of Eq. (2.15). For certain ranges, the power law exponent m *is independent of temperature and pressure* (since the master curve is independent of temperature and pressure), but it slowly increases with higher values of $\dot{\gamma}\eta_0$ ranges. The pressure and temperature dependence of the viscosity η is comprised by the pressure- and temperature-dependent zero viscosity η_0 only. The pressure coefficient α, the temperature coefficient β, and the activation energy E of the viscosity in the power law region are then related to

TABLE IV

ACTIVATION ENERGY E_0 AND PRESSURE COEFFICIENT α_0 OF THE ZERO VISCOSITY η_0[a]

Polymer	E_0 [10^4 J/gm mole]	α_0 [10^{-8} m^2 N^{-1}]	Literature
l.d.PE	5.44	—	[28]
h.d.PE	7.08–8.99	3.25–3.98	[33]
PS	—	4.28–9.07	[32]
PMMA	14.23–19.13	2.45–4.08	[33]

[a] The temperature coefficient β_0 of the zero viscosity around the temperature T_0 is equal to E_0/RT_0^2, see Eq. (2.13). α and β of the power law region can be determined from α_0 and β_0 by dividing with m, see Eq. (2.19).

α_0, β_0, and E_0 of the zero viscosity by

$$\alpha = \alpha_0/m, \qquad \beta = \beta_0/m, \qquad E = E_0/m. \tag{2.19}$$

Table IV [28, 32, 33] lists E_0 and α_0 values of some polymers; the data can be used to determine α and β of the power law which describes the viscosity in the $\dot{\gamma}\eta_0$ range of the application in question. Semjonow [29] collected E_0 data from the literature which is quite extensive.

Due to the small values of α, the pressure dependence of the viscosity usually can be neglected up to moderate pressure levels (<300 bar, depending on the value of α) as they occur in extrusion. In injection molding studies, however, the pressure may adopt values up to 1500 bar and the pressure dependence should be included. *In the following study, the pressure dependence of viscosity is not taken into consideration,* although the numerical procedure would not have to be much different: it just would require one or more iterations of the whole computation procedure, until the axial pressure profile along the channel is known.

The concept of steady shear flow is a theoretical one and it can only be approximated. However, the rheological properties of molten polymers do not seem to be too sensitive to some deviation from steady shear flow; and for a large number of applications, the results from steady shear flow calculations agree with flow experiments reasonably well. The shear flow might be *unsteady* ($\partial/\partial t \neq 0$); during startups a constant stress is achieved only after some time of development. But even if the flow is steady ($\partial/\partial t = 0$), it still might deviate from shear. Deviations occur as slowly relaxing entrance effects; temperature *changes along stream lines,* which induce changes in shear rate, are in contradiction to "steady shear flow," which is defined to be isothermal and at constant shear rate; in Poiseuille flow, pressure changes

actually influence the density, while the fluid supposedly is incompressible. Flows of this kind are called *nearly steady shear flows*, where the adverb *nearly* may refer to the word *steady* or the word *shear*. These limitations of the applicability of the shear flow concept will be mentioned again, when all the assumptions are listed together with the system of equations, see Sections II.B.1 and II.C.1.

Shear Flow Geometries with Open or with Closed Stream Lines

The most important shear flow geometries are shown in Fig. 3; Table V [34–95] lists heat transfer studies on those flow geometries. The flow due to the relative motion of one of the surfaces is called *Couette flow*, while

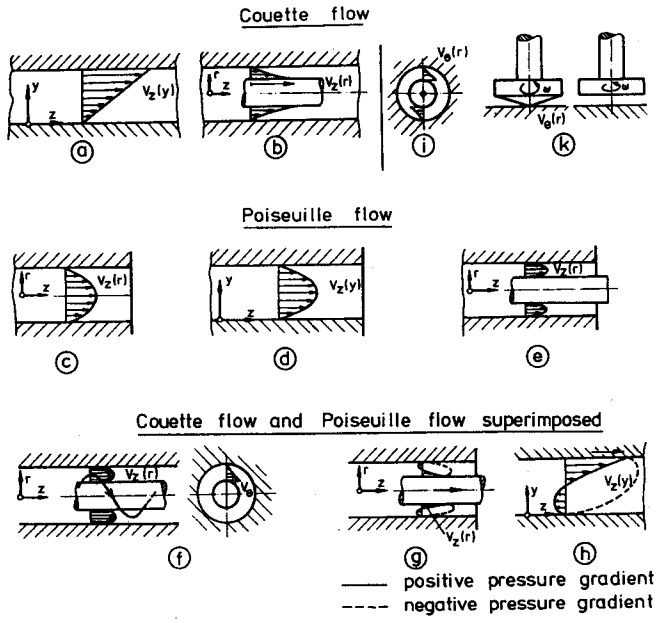

FIG. 3. The main simple shear flow geometries [2]: (a) drag flow in the narrow slit between two parallel plates (plane Couette flow), no pressure gradient; (b) axial drag flow between two coaxial cylinders (annular Couette flow), no pressure gradient; (c) flow through a pipe with constant circular cross section (Poiseuille flow); (d) flow through a narrow slit (Poiseuille flow); (e) axial flow through an annulus (Poiseuille flow); (f) helical flow (flow through an annulus with rotating inner cylinder); (g) axial drag flow in an annulus with nonzero axial pressure gradient; (h) drag flow in the narrow slit between two parallel plates with nonzero pressure gradient; (i) angular drag flow in the annulus between two coaxial cylinders (circular Couette flow), no pressure gradient; (k) flow in a cone-and-plate or in a plate-and-plate viscometer. Geometry a will be referred to as a_1 if the stream lines are open, or a_2 if the stream lines are closed (limiting case $\kappa \to 1$ of geometry i).

TABLE V: Heat Transfer Studies in Steady Shear Flow

Temperature field	Thermal boundary condition	Flow geometries with open stream lines								Flow geometries with closed stream lines		
		a_1	b	c	d	e	f	g	h	a_2	i	k
Fully developed	constant wall temperature	see a_2		34–41	35, 37, 42				43	37, 38, 42, 44–48	38, 42, 45, 49–51E	52, 53E, 54
	constant heat flux at wall, adiabatic wall											
	mixed	see a_2		55E	42					38, 42, 45, 46, 55E, 56, 57E	38, 45, 49, 51E, 55E, 58E, 59E	54
Developing	constant wall temperature	60, 61		62–64, 65E, 66, 67E, 68E, 69–71, 72E, 73, 74, 75E, 76–79, 133	77, 80–82	77, 83	82, 84, 85			86E, 87, 88		
	constant heat flux at wall, adiabatic			63, 67E, 68E, 70, 71, 72E, 76, 78, 79		83				89		
	mixed			90E, 93E, 94E, 95E	77, 90E,	77, 90E,	84, 85, 91E			89, 92		

[a] Letters $a, b, \ldots, k$ refer to Fig. 3, where flow geometry a occurs with open and with closed stream lines. The numbers refer to the list of literature. Experimental studies or studies which contain experiments are marked with an E.

the flow due to a pressure gradient is called *Poiseuille flow*. In the literature, most emphasis has been laid on the fully developed temperature field in pipe flow and in Couette flow, and on the developing temperature field in pipes with circular cross section. Experimental studies or studies that contain an experimental part are marked by an E. Poiseuille flow in a pipe with constant but irregular cross section or Poiseuille flow in curved channels with constant cross section induce some small secondary flow in the cross section [96]; this will be mentioned in Section III on nonviscometric flow.

A detailed description of the historical development of shear flow analysis can be found in the introduction of original papers on the different problems (see for instance [55] for the fully developed temperature profiles and [77, 78] for developing temperature profiles in pipe flow). This study tries to describe the various aspects of shear flow analysis and give credit to the different authors in connection with the arguments in the analysis.

Stream lines are lines whose tangents are everywhere parallel to the velocity vectors. In steady flow, the stream lines describe the paths of fluid elements. The heat transfer in the various shear flow geometries depends on whether the stream lines are open (type a_1–h in Fig. 3) or closed (type a_2, i, k in Fig. 3). In steady flows with *open* stream lines, the temperature is locally constant with time ($\partial T/\partial t = 0$); for displacements along the flow direction, however, it changes until a fully developed temperature field ($DT/Dt = 0$ for $T_w = \text{const}$) is reached, where conduction and viscous dissipation balance. In processing equipment, the fully developed temperature field is achieved rarely since the flow channels are not long enough and the thermal boundary conditions usually change in the flow direction. Nevertheless, the calculated fully developed temperature field is very useful as a reference state. The degree of development can be estimated from the value of the *Graetz number*. The unsteady developing temperature ($\partial T/\partial t \neq 0$, $\partial T/\partial z \neq 0$) in flows with open stream lines has been studied very little, possibly because the numerical or experimental techniques are very involved.

In shear flows with *closed* stream lines, the temperature is assumed to be uniform along the stream lines, but locally changing with time ($\partial T/\partial \Theta = 0$; $\partial T/\partial t \neq 0$) during the starting phase. The stream lines are supposed to be circles, and Θ is the coordinate in the flow direction. Convective heat transfer has no influence on the temperature field. After some developing time, a constant temperature field is reached where viscous dissipation and conduction balance. The degree of development can be estimated from the value of the *Fourier number*.

Drag flow in a narrow slit (plane Couette flow) is introduced twice (a_1 and a_2 in Table V). One might treat it as an entrance value problem (as in a_1) and study the axial development of the temperature field beginning from

some inlet temperature distribution. On the other hand, one might treat plane Couette flow as a limiting case of circular Couette flow (as in a_2); i.e., the stream lines are thought to be closed, and there are no changes in flow direction ($\partial/\partial\Theta = 0$). The temperature develops with time, beginning with some initial temperature distribution. The fully developed temperature field is the same for both cases.

A. THERMAL BOUNDARY CONDITION

The specific heat flux q at the boundary is given by the thermal conductivity k_{fluid} of the fluid together with the temperature gradient $(\partial T/\partial r)_w$ in the fluid layer next to the wall

$$q = -k_{\text{fluid}}(\partial T/\partial r)_w. \tag{2.20}$$

The problems of this section are described in cylindrical coordinates z, r, Θ, where r is the coordinate perpendicular to the wall.

If the thermal boundaries are not taken to be isothermal ($T_w \neq$ const), the thermal development in the fluid is connected with the thermal development in the wall. The heat flux at the boundary is determined not only by the conduction to the outside of the channel, but also by the thermal capacity of the wall. Both effects will be analyzed separately in the following.

1. *Biot Number and Conduction to Surroundings*

If the effect of energy storage in the wall is of no influence, the heat flux at the boundary generally depends on the difference of the temperature level of the experiment to some temperature of the surroundings. In the analysis, the temperature gradient in the fluid layer next to the wall is taken to be proportional to the outer temperature difference $(T_s - T_w)$; T_s is the temperature of the surroundings, and T_w is the wall temperature, i.e., the temperature at the boundary between melt and containing wall. The coefficient of proportionality is the Biot number [69, 71] of equation

$$(\partial T/\partial r)_w = \text{Bi}(T_s - T_w)/h. \tag{2.21}$$

Bi is already well known for describing the thermal boundary condition during the heating or cooling of *solid* bodies (see for instance [97, 98]). h is a characteristic length of the flow channel, i.e., the gap width of a slit or the radius of a pipe.

Equation (2.21) describes just the radial heat flux in the wall; the axial heat conduction in the wall is neglected in the Biot number. For shear flow applications with *closed* stream lines, the validity of this assumption has to be verified in each case. However, the assumption seems to be reasonable

for shear flow applications with *open* stream lines, where the axial temperature gradient is much smaller than the radial one; during thermal development, the heat flux into the wall changes in the flow direction, but beyond a certain distance from entrance into the channel, these changes are small due to a small axial gradient.

The value of Bi for certain applications can be derived from a heat balance for the wall. *In some cases* Bi *is a function of geometry and of the thermal conductivities only.* The heat flux through the wall of a pipe, for instance, can be determined from the inner radius r_p of the pipe wall, the wall thickness s, the thermal conductivity k_{wall}, and the inner and outer temperatures T_1 and T_2 [98, p. 71].

$$q = \frac{k_{wall}}{r_p} \frac{T_1 - T_2}{\ln(1 + s/r_p)}. \tag{2.22}$$

On the other hand, the heat flux into the wall is determined by the thermal boundary condition (Eqs. (2.20) and (2.21))

$$q = -k_{fluid}\left(\frac{\partial T}{\partial r}\right)_w = -k_{fluid}\frac{Bi}{r_p}(T_s - T_w). \tag{2.23}$$

Thus, for steady pipe flow with *controlled temperature at the outer wall* ($T_1 = T_w$; $T_2 = T_s$), the *Biot number can be calculated* by equating Eqs. (2.22) and (2.23):

$$Bi_{pipe} = \frac{k_{wall}}{k_{fluid}} \frac{1}{\ln(1 + s/r_p)}. \tag{2.24}$$

Applying this formula to capillary viscometry ($r_p = 0.5$ cm, $s = 4.5$ cm), one finds values of Bi $\approx$ 20. Examples for pipe flow with $1 \leq Bi \leq 100$ are given in Fig. 8 of Section II.B.4. Similarly, the outer Biot number Bi_a for annular flow (with r_i and r_a as the inner and outer radius) would be

$$Bi_{a,\,annulus} = \frac{k_{wall}}{k_{fluid}} \frac{1 - r_i/r_a}{\ln(1 + s/r_a)}, \tag{2.25}$$

and some examples for pipe extrusion give $1 < Bi_a < 10$.

Figure 4 illustrates the geometrical meaning of Bi. The tangent to the temperature curve $T(r/h)$ at the wall passes through a guide point outside the flow channel; the distance between the guide point and the wall is Bi^{-1}, and the ordinate is the surrounding temperature T_s. For Bi = 10, for instance, the distance of the guide point from the boundary is 1/10 of the gap width h for annular flow or 1/10 of the radius r_a for pipe flow. When the Biot number changes in flow direction, one can visualize this by the appropriate displacement of the guide point.

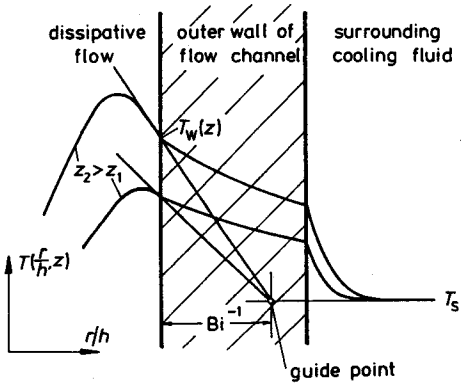

FIG. 4. Thermal boundary condition for channel flow described by the Biot number Bi and the surrounding temperature T_s, i.e., by a guide point outside the channel.

The boundary condition for the temperature field is not known in general. If there are temperature data $T_w(z)$ available, they can be used in a numerical program. But often one has to guess these conditions to make an estimate of the temperature profiles possible. Most of the studies shown in Table V prescribe idealized conditions such as:

constant wall temperature

$$T_w = \text{const} \quad \text{or} \quad \text{Bi}_i \to -\infty, \quad \text{Bi}_a \to \infty; \quad \text{(guide point at the wall)},$$

constant heat flux at wall

$$(\partial T/\partial r)_w = \text{const} \quad \text{or} \quad \text{Bi}(T_s - T_w) = \text{const},$$

adiabatic wall

$$(\partial T/\partial r)_w = 0 \quad \text{or} \quad \text{Bi} = 0; \quad \text{(guide point at infinity)}.$$

The use of the Biot number allows one to adopt more realistic thermal boundary conditions, and one goal of further experimental heat transfer studies should be the measurement of Bi in various engineering applications.

For the examples shown throughout this analysis, the *boundary condition at the wall will be described by* Bi *and* T_s *independent of* z (for steady flow with *open* stream lines) or independent of t (for flow with *closed* stream lines), respectively. If the value of Bi is finite, the wall temperature $T_w(z)$ or $T_w(t)$ changes according to the development of the temperature field, and it reaches a constant value $T_{w,\infty}$ in the fully developed temperature field.

2. *Thermal Capacity of the Wall*

The Biot number is appropriate for describing heat conduction to the surroundings. However, if the wall stores some energy during thermal development, a different boundary condition is needed to describe this effect.

The thermal development should be calculated for the fluid and the wall together. This has been done by Powell and Middleman [92] for plane Couette flow with one wall having a finite mass, which absorbs part of the heat generated by viscous dissipation. The thermal development was found to be significantly retarded by the response of the boundary; the parameter characterizing the retardation is the ratio of mass times heat capacity of the solid wall and that of the fluid: $(mc_p)_{\text{wall}}/(mc_p)_{\text{fluid}}$.

In this study, however, detailed calculation of the temperature field in the wall will be avoided by *introducing a capacitance parameter C*. For flow with *closed* stream lines, the wall temperature changes with time during the thermal development. The rate of thermal energy stored in the wall is assumed to be proportional to the time change DT_w/Dt of the temperature at the boundary. The temperature gradient in the fluid layer near the wall becomes

$$\left(\frac{\partial T}{\partial r}\right)_w = \text{Bi}\,\frac{T_s - T_w}{h} \underset{(+)}{-} C\,\frac{h}{a_{\text{fluid}}}\,\frac{DT_w}{Dt} \tag{2.26}$$

The capacitance parameter C is dimensionless, and the ratio h/a_{fluid} is used in Eq. (2.26) because below the whole boundary condition will be made dimensionless. C is determined by the geometry and by the capacitance of both the fluid and the wall. The heat flux to the surroundings is kept proportional to the outer temperature difference $T_s - T_w$.

Assuming constant thermal properties of the wall material, the rate of energy storage in the wall is proportional to the time change of the average temperature of the whole wall. The time change of the average temperature of the wall might not be proportional to the time change DT_w/Dt at the boundary. Thus, the capacitance parameter describes the effect of energy storage in the wall only approximately. In many polymer engineering applications, however, the thermal development in the wall is much faster than the thermal development in the fluid, and the temperature at the boundary is representative for the whole wall. An example where uniform temperature in the wall is assumed will be given in the following.

Example for C: The temperature of the inner cylinder of a Couette system (geometry i in Fig. 3, r_i = inner radius, r_a = outer radius, $h = r_a - r_i$) changes during the thermal development of a shear experiment. The temperature of the inner cylinder is assumed to be uniform and equal to the

temperature at the boundary; this is justified, if the ratio of the Fourier numbers (see Section II.C.2) is small:

$$\frac{a_{\text{cylinder}}}{a_{\text{fluid}}}\left(\frac{r_a - r_i}{r_i}\right)^2 \gg 1. \tag{2.27}$$

Axial heat conduction is neglected and, of course, the Biot number is equal to zero. The heat flux into the inner cylinder is balanced by the temperature raise of the inner cylinder:

$$2\pi r_i(\partial T/\partial r)_w\, k_{\text{fluid}} = \pi r_i^2(\rho c)_{\text{cylinder}}\, \partial T_w/\partial t. \tag{2.28}$$

By comparing Eq. (2.28) with Eq. (2.26) one finds the capacitance parameter for the Couette system:

$$C = \frac{r_i}{2(r_a - r_i)}\frac{(\rho c)_{\text{cylinder}}}{(\rho c)_{\text{fluid}}}. \tag{2.29}$$

The influence of C on the thermal development will be shown in Figs. 23 and 24 of Section II.C.3.

For most of the steady heat transfer problems with *open* streamlines, the walls are stationary or just rotating about the z axis. The capacitance of the wall has no influence on the temperature ($DT_w/Dt = 0$). An exception would be the inner boundary of axial Couette flow (geometry b or g of Fig. 3) as occurs in the wire coating die. The corresponding thermal boundary condition is

$$\left(\frac{\partial T}{\partial r}\right)_w = \text{Bi}_i\frac{T_s - T_w}{h} + C_i\frac{v_w h}{a_{\text{fluid}}}\frac{\partial T_w}{\partial z}. \tag{2.30}$$

v_w is the axial velocity of the wall (inner cylinder).

For the example of a wire coating process, a heat balance for the inner cylinder (wire) leads to the same formula for the capacitance parameter as for the Couette system above, Eq. (2.29). The assumptions made were uniform temperature in cross section of wire and no axial conduction in the wire. The Biot number for the wire is zero.

The geometrical meaning of the boundary condition with capacity and conduction to the surroundings is shown in Fig. 5. The guide point is not at a constant position (as for flow with $DT_w/Dt = 0$; see Fig. 4), but moves during the thermal development along $T_s = \text{const}$. For the fully developed temperature field, the wall temperature does not change any more; the capacitance of the wall is of no influence, and the guide point is, as in Fig. 4, at a distance Bi^{-1} from the boundary.

An adiabatic or perfectly insulating wall would be a wall without thermal capacitance (or with an appropriate heat source of its own); the corresponding Biot number and the capacitance parameter are both equal to zero.

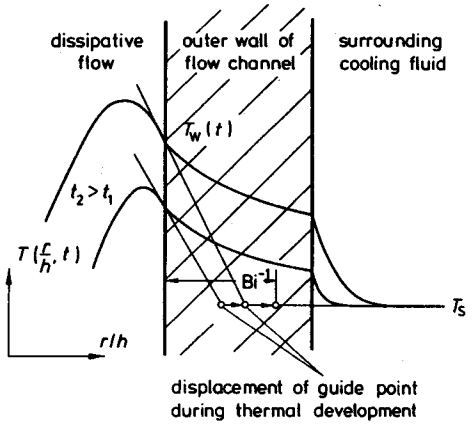

FIG. 5. Thermal boundary condition for a wall with thermal capacitance. During the thermal development, the guide point of the tangent on the temperature field moves toward the position (Bi^{-1}, T_s).

B. STEADY SHEAR FLOW WITH OPEN STREAM LINES

Steady shear flow with open stream lines could be analyzed now by going into each of the shear flow geometries a_1–h in Fig. 3. Instead, it will be demonstrated here that the helical flow geometry is representative since all the other geometries are limiting cases of helical flow.

In helical flow, the fluid flows through an annulus between two concentric cylinders (Fig. 6). Axially, the fluid flows due to a pressure gradient and/or due to the axial movement of the inner (or outer) cylinder. In the circumferential direction, the fluid flows due to the rotation of the inner cylinder. Fluid elements move on helical paths; the angle of the helices

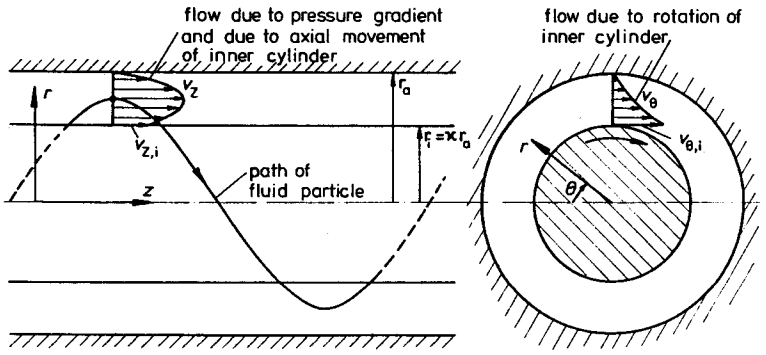

FIG. 6. Helical flow geometry.

depends on the ratio of the axial to the circumferential velocity component, which both depend on the radial position of the fluid element.

The annular geometry is characterized by the ratio of the radii

$$\kappa = r_i/r_a. \tag{2.31}$$

The limiting cases are the pipe ($\kappa = 0$) and the plane slit ($\kappa \to 1$). The position in the annulus is given by dimensionless coordinates:

$$\text{radially:} \quad Y = \frac{r - r_i}{r_a - r_i}, \qquad 0 \leq Y \leq 1; \tag{2.32}$$

$$\text{axially:} \quad Z = \frac{z}{l\,\mathrm{Gz}}, \qquad 0 \leq Z \leq \mathrm{Gz}^{-1}. \tag{2.33}$$

The value of Z indicates, as will be shown in the following, to what degree the temperature field is developed along the channel. The Graetz number Gz will be defined in Eq. (2.56).

1. *Assumptions and System of Equations*

The equations of change, Eqs. (1.1)–(1.3), have to be simplified before they can be solved. First the assumptions will be listed, then they will be commented upon:

incompressible fluid with constant thermal conductivity and diffusivity;
steady laminar flow ($\partial/\partial t = 0$);
rotational symmetry ($\partial/\partial\Theta = 0$);
velocity gradients

$$\frac{\partial v_z}{\partial z}, \frac{\partial v_\Theta}{\partial z}, \frac{\partial v_r}{\partial z}, \frac{\partial v_r}{\partial r}, \frac{v_r}{r} \ll \frac{\partial v_z}{\partial r}, r\frac{\partial}{\partial r}\left(\frac{v_\Theta}{r}\right);$$

no slip at walls;
inertia negligible; kinematically developed velocity at $z = 0$;
gravity negligible;
viscosity measured at constant temperatures and constant shear rates gives applicable local values of the viscosity during temperature changes and during small changes in shear rate; rheologically developed stress at $z = 0$;
convective heat transfer much larger than conduction in flow direction;
heat transport toward the walls by conduction only.

Throughout this section the molten polymer is taken to have constant density ($\rho/\bar{\rho} = 1$; $\epsilon = 0$), constant thermal conductivity ($k/\bar{k} = 1$), and constant thermal diffusivity ($a/\bar{a} = 1$). In the general system of equations for helical flow, however, these properties have been kept as variables, and one might

evaluate them in the numerical program using $\rho(p, T)$, $k(p, T)$, and $a(p, T)$ data from measurements on the fluid at rest.

The density is assumed to be constant since in actual experiments (with $T \neq$ const, $p \neq$ const) density changes are delayed, i.e., the changes are overestimated if one applies ρ data of equilibrium thermodynamics. For this reason, the *effect of expansion cooling is not considered* in all but one example. For the one exception, the supposed expansion cooling term (containing ϵT) of Eq. (1.8) is kept in brackets in the energy equation; the effect of expansion cooling is estimated in an example of pipe flow; see Fig. 13 with $\epsilon \neq 0$.

During the axial development of the temperature field, the temperature-dependent viscosity is changing and causes the shape of the velocity profiles to change accordingly. For continuity reasons, the changes of the axial velocity require some radial flow. Using the equation of continuity, Eq. (1.1), the radial velocity components have been estimated from the change of the axial velocity component and have been found to be small ($|v_r| < 10^{-2}\,\bar{v}$). Throughout Section II.B, the influence of the radial velocity components on the radial heat transfer, on dissipation, and on the viscosity will therefore be neglected.

Due to rotational symmetry and due to $\partial v_z/\partial r$ and $r\,\partial(v_\Theta/r)/\partial r$ being the largest gradients, the isotropic pressure is taken to be a function of z only:

$$p = p(z).$$

The shear rate becomes

$$\dot{\gamma} = \left[\left(r\frac{\partial}{\partial r}\left(\frac{v_\Theta}{r}\right)\right)^2 + \left(\frac{\partial v_z}{\partial r}\right)^2\right]^{1/2}, \tag{2.34}$$

which is the root of the second invariant of the rate of strain tensor.

In most applications, molten polymers do not slip at the wall, and in all the published heat transfer studies this assumption has been made. Polymeric materials such as high density polyethylene, polyvinylchloride, or polybutadiene, however, seem to slip in certain ranges of the normal stress and shear stress at the wall [99, 100]; the velocity field is then drastically changed and additional frictional heating occurs on the sliding surfaces.

The velocity at the entrance ($z = 0$) is assumed to be fully developed; i.e., inertial effects are neglected, and the stress is assumed to be governed by the three viscometric functions (of steady unidirectional shear flow) at the local shear rate and the local temperature. For low Reynolds number pipe flow of *inelastic* liquids, the kinematic development is practically completed after a length of $l = 0.1 r_a\,\mathrm{Re}$ [101]. Neglecting inertia might therefore be justified for entrance flow of molten polymers, which is low Reynolds number flow.

The rheological properties of the polymer entering the annulus are determined by a flow and temperature history, which obviously is different from that for steady shear flow. Judging from the measured pressure profiles along a slit die, steady shear flow might be reached practically at $l/h = 20$–30 (depending on geometry, flow rate, and polymer melt). Therefore, the heat transfer study of this section may give unrealistic results for flow in short annuli and short circular holes, which rheologically should be treated as an entrance flow problem.

The equations for conservation of mass, momentum, and energy in helical flow are

$$0 = \frac{1}{r}\frac{\partial}{\partial r}(\rho r v_r) + \frac{\partial}{\partial z}(\rho v_z),$$

$$0 = \frac{\partial}{\partial r}\left[r^3\eta\,\frac{\partial}{\partial r}\left(\frac{v_\Theta}{r}\right)\right],$$

$$0 = -\frac{\partial p}{\partial z} + \frac{\partial}{r\,\partial r}\left(r\eta\,\frac{\partial v_z}{\partial r}\right), \tag{2.35}$$

$$\rho c v_z \frac{\partial T}{\partial z} = \frac{\partial}{r\,\partial r}\left(rk\,\frac{\partial T}{\partial r}\right) + \left[T\epsilon v_z \frac{\partial p}{\partial z}\right] + \eta\left[\left(r\frac{\partial}{\partial r}\frac{v_\Theta}{r}\right)^2 + \left(\frac{\partial v_z}{\partial r}\right)^2\right].$$

The average axial velocity is

$$\bar{v}_z = \frac{2}{r_a^2 - r_i^2}\int_{r_i}^{r_a} \frac{\rho}{\bar{\rho}}\, v_z r\, dr. \tag{2.36}$$

The initial and the boundary conditions are

$$\left.\begin{aligned} T(r,0) &= T_e(r)\\ v_r(r,0) &= 0\\ v_\Theta(r,0) &= v_{\Theta,e}(r)\\ v_z(r,0) &= v_{z,e}(r)\end{aligned}\right\} \quad r_i \le r \le r_a, \tag{2.37}$$

$$\left.\begin{aligned} \frac{\partial T(r_i,z)}{\partial r} &= \mathrm{Bi}_i\,\frac{T_{s,i} - T(r_i,z)}{h}\\ \frac{\partial T(r_a,z)}{\partial r} &= \mathrm{Bi}_a\,\frac{T_{s,a} - T(r_a,z)}{h}\\ v_r(r_i,z) &= v_r(r_a,z) = 0\\ v_\Theta(r_i,z) &= v_{\Theta,i};\ v_\Theta(r_a,z) = 0\\ v_z(r_i,z) &= v_{z,i};\ v_z(r_a,z) = v_{z,a}\end{aligned}\right\} \quad 0 < Z \le l.$$

The meanings of Bi and T_s have been described already in Section II.A on the thermal boundary condition ($Bi_i < 0$; $Bi_a > 0$). The capacitance parameter C of Eq. (2.30) has been omitted here since the temperatures are assumed to be steady and since the walls are stationary for most shear flow applications with open stream lines.

For the dimensionless presentation of the equations, a reference velocity $\bar{v}$ can be defined by vector addition of the mean axial velocity $\bar{v}_z$ and the mean circumferential velocity $v_{\Theta,i}/2$:

$$\bar{v} = [\bar{v}_z^2 + (v_{\Theta,i}/2)^2]^{1/2}. \tag{2.38}$$

The reference length is taken to be the gap width

$$h = r_a - r_i. \tag{2.39}$$

For pipe flow the reference length becomes equal to the pipe radius ($h = r_a$).

Using the reference velocity $\bar{v}$ and the reference length h, one can define a reference shear rate

$$\bar{\dot{\gamma}} = \bar{v}/h \tag{2.40}$$

and a reference viscosity

$$\bar{\eta} = \eta(\bar{\dot{\gamma}}, T_0). \tag{2.41}$$

T_0 is a characteristic temperature level of the experiment, for instance the average melt temperature at the inlet ($T_0 = T_e$). Flow problems with viscous dissipation do not have a characteristic temperature difference $(\Delta T)_{ref}$ to which temperature changes can be related. Some authors relate the temperature to the temperature level T_0; this, however, seems to be rather arbitrary since T/T_0 might assume different values in otherwise similar processes (e.g., at different temperature levels T_0 and T_0'). The value of T/T_0 additionally depends on the choice of temperature scale. Therefore, the temperature coefficient of the most temperature-sensitive property, the viscosity, has been used to define the dimensionless temperature: $(\Delta T)_{ref} = \beta^{-1}$.

The dimensionless variables are:

velocity
$$(V_R, V_\Theta, V_Z) = (v_r/\bar{v}, v_\Theta/\bar{v}, v_z/\bar{v}), \tag{2.42}$$

pressure gradient
$$P' = \frac{\partial p}{\partial z}\frac{h^2}{\bar{\eta}\bar{v}}, \tag{2.43}$$

shear stress
$$P_{RZ} = \tau_{rz}\frac{h}{\bar{\eta}\bar{v}}, \tag{2.44}$$

$$P_{R\Theta} = \tau_{r\Theta}\frac{h}{\bar{\eta}\bar{v}}, \tag{2.45}$$

radial position
$$R = r/r_a = (1 - \kappa)r/h; \quad \kappa \le R \le 1, \tag{2.46}$$

viscosity
$$\frac{\eta}{\bar{\eta}} = \left(\frac{\dot{\gamma}}{\bar{\dot{\gamma}}}\right)^{(1/m)-1} \exp(-\beta(T - T_0)), \tag{2.47}$$

temperature
$$\vartheta = \beta(T - T_0) = (T - T_0)/(\Delta T)_{\text{ref}}. \tag{2.48}$$

The dimensionless form of the equations becomes

$$0 = \frac{\partial}{R\,\partial R}\left(\frac{\rho}{\bar{\rho}} R V_R\right) + \frac{r_a}{l\,\mathrm{Gz}}\frac{\partial}{\partial Z}\left(\frac{\rho}{\bar{\rho}} V_Z\right), \tag{2.49}$$

$$0 = \frac{\partial}{\partial R}\left[R^3 \frac{\eta}{\bar{\eta}}\frac{\partial}{\partial R}\frac{V_\Theta}{R}\right], \tag{2.50}$$

$$0 = \frac{-P'}{(1-\kappa)^2} + \frac{\partial}{R\,\partial R}\left[R\frac{\eta}{\bar{\eta}}\frac{\partial V_Z}{\partial R}\right], \tag{2.51}$$

$$\frac{\rho c V_Z}{\bar{\rho}\bar{c}\bar{V}_Z}\frac{\partial \vartheta}{\partial Z} = (1-\kappa)^2 \frac{\partial}{R\,\partial R}\left(\frac{k}{\bar{k}} R \frac{\partial \vartheta}{\partial R}\right) + [\mathrm{Na}\,\epsilon T V_Z P'] + \mathrm{Na}\frac{\eta}{\bar{\eta}}(1-\kappa)^2\left[\left(R\frac{\partial}{\partial R}\frac{V_\Theta}{R}\right)^2 + \left(\frac{\partial V_Z}{\partial R}\right)^2\right]. \tag{2.52}$$

The dimensionless average axial velocity is

$$\bar{V}_Z = \frac{2}{1-\kappa^2}\int_\kappa^1 \frac{\rho}{\bar{\rho}} V_Z R\, dR, \tag{2.53}$$

and the initial and boundary conditions are

$$\left.\begin{aligned} &\vartheta(R,0) = \beta(T_e(r) - T_0) = \vartheta_e(R)\\ &V_R(R,0) = 0\\ &V_\Theta(R,0) = V_{\Theta,e}(R) = v_{\Theta,e}(r)/\bar{v}\\ &V_Z(R,0) = V_{Z,e}(R) = v_{z,e}(r)/\bar{v} \end{aligned}\right\} \quad \kappa \le R \le 1,$$

$$\left.\begin{aligned} &\frac{\partial \vartheta(\kappa,Z)}{\partial R} = \mathrm{Bi}_i\frac{\vartheta_{s,i} - \vartheta(\kappa,Z)}{1-\kappa}\\ &\frac{\partial \vartheta(1,Z)}{\partial R} = \mathrm{Bi}_a\frac{\vartheta_{s,a} - \vartheta(1,Z)}{1-\kappa}\\ &V_R(\kappa,Z) = V_R(1,Z) = 0\\ &V_\Theta(\kappa,Z) = v_{\Theta,i}/\bar{v};\ V_\Theta(1,Z) = 0\\ &V_Z(\kappa,Z) = v_{z,i}/\bar{v};\ V_Z(1,Z) = v_{z,a}/\bar{v} \end{aligned}\right\} \quad 0 < Z \le \mathrm{Gz}^{-1}. \tag{2.54}$$

In the expansion cooling term of the energy equation, the absolute temperature T is not replaced by the dimensionless temperature ϑ since the dimensionless product ϵT can be considered as constant within the accuracy of the calculations.

The system of equations is formulated in cylindrical coordinates, and $R = r/r_a$ is kept as a dimensionless coordinate, even if $h = r_a - r_i$ is the reference length and not r_a. The results are presented using the dimensionless coordinate Y. If one wants to avoid this inconsistency, the substitution

$$R = Y(1 - \kappa) + \kappa, \qquad \partial R = \partial Y(1 - \kappa)$$

eliminates R from the equations; with this substitution the equations look unnecessarily complicated and therefore both coordinates are kept: R in the equations and Y in the graphical presentation of the results. For pipe flow, R and Y are identical.

2. *Dimensionless Parameters*

The problem as stated in Eqs. (2.49)–(2.54) is completely determined by six dimensionless parameters (Na, Gz, κ, m, $\bar{V}_Z$, L) together with the boundary conditions. A general description of the dimensionless parameters has been given by Pearson [3]. If the pressure dependence of the viscosity or nonconstant thermal properties would be included, the number of parameters would increase accordingly.

The equation of motion and the equation of energy, Eqs. (2.35), are coupled by the temperature-dependent viscosity. The extent of the coupling increases with the value of the Nahme number [44]:

$$\text{Na} = \beta \bar{v}^2 \bar{\eta}/\bar{k} \tag{2.55}$$

which compares the dissipation term with the conduction term in the equation of energy. For values of Na greater than 0.1–0.5 (depending on geometry and thermal boundary conditions), the viscous dissipation leads to significant viscosity changes, i.e., changes reflected in the T and v fields. For smaller values of Na, isothermal conditions can be achieved practically; in this case, the equation of motion can be integrated independently of the energy equation.

In some studies the Brinkman number [62] $\text{Br} = \bar{v}^2 \bar{\eta}/kT_0$ has been used instead of the Nahme number. However, Br contains the arbitrary temperature level T_0 (since no characteristic temperature difference is available) and may, therefore, have very different values for similar processes. The value of Br does not give any information on the extent of the coupling between the equation of motion and the energy equation. (Note that the Nahme number sometimes is called the Griffith number after Griffith [102], who used the same dimensionless group in one of the later applications.)

The energy equation contains a convection, a conduction, and a dissipation term. By comparing the convection and the conduction terms one arrives at the Graetz number [103]

$$\mathrm{Gz} = \bar{v}_z h^2/\bar{a}l \tag{2.56}$$

which has been included in the dimensionless form of the z coordinate. The Graetz number can be understood to be the ratio of the time required for heat conduction from the center of the channel to the wall and the average residence time in the channel [75]. A large value of Gz means that heat convection in flow direction is more important than conduction toward the walls, Gz = 100, for instance, is a common value for extruder dies. (Note that some authors define the Graetz number $\mathrm{Gz} \cdot \pi$.)

The Gz number has been defined with the average axial velocity and the length of the annulus, instead of the reference velocity $\bar{v}$ and some mean path length $\bar{l}$ for the fluid elements in the annular section. One might, however, define $\bar{l}$ to be $\bar{l} = l\bar{v}/\bar{v}_z$ which would result in a Graetz number $\mathrm{Gz} = \bar{v}h^2/a\bar{l}$ equal to the one defined in Eq. (2.56).

The value of the dimensionless average axial velocity

$$\bar{V}_Z = \frac{\bar{v}_z}{\bar{v}} = \left[1 + \left(\frac{v_{\theta,i}}{2\bar{v}_z}\right)^2\right]^{-1/2}, \qquad 0 \le \bar{V}_Z \le 1, \tag{2.57}$$

describes whether the flow tends to be closer to axial flow in an annulus ($\bar{V}_Z = 1$) or closer to circular Couette flow ($\bar{V}_Z = 0$).

The dimensionless length of the annulus is

$$L = l/h = l/(r_a - r_i). \tag{2.58}$$

Another dimensionless parameter originates from the shear dependence of the viscosity: the power law exponent m in Eq. (2.47).

3. *Universal Numerical Shear Flow Program*

The system of equations is solved by an iterative implicit method ($\partial/\partial Z$ described by a backward difference; $\partial/\partial R$ and $\partial^2/\partial R^2$ described by center differences; gradients at a boundary are calculated from a parabola through three points), similar to the one used in an earlier study on helical flow [85]. A network is superimposed on the annulus. Difference equations are then derived for each node point, which fulfill the condition of conservations of mass, momentum, and energy. The method described in the following was found to converge rapidly; for example, a run with 60 radial and 250 axial steps requires a computation time of about 30 s.

The solution procedure is an iterative one, in which the coupled equations are linearized and solved separately. The nonlinear terms and the coupling

conditions have to be satisfied by alternating improvements on the velocity and on the temperature field. The iteration is terminated when the relative change in successive steps becomes smaller than one thousandth ($\Delta_{rel} < 10^{-3}$).

The flow chart in Fig. 7 describes the structure of the program. The *velocity field at the entrance*, which is assumed to be fully developed kinematically, is calculated by taking, as a first guess, a Newtonian viscosity according to the entrance temperature field. The shear dependence of viscosity is included then by iteration, using the improved values of the velocity field. After about 6–20 iterations, the velocities reach values that are practically constant.

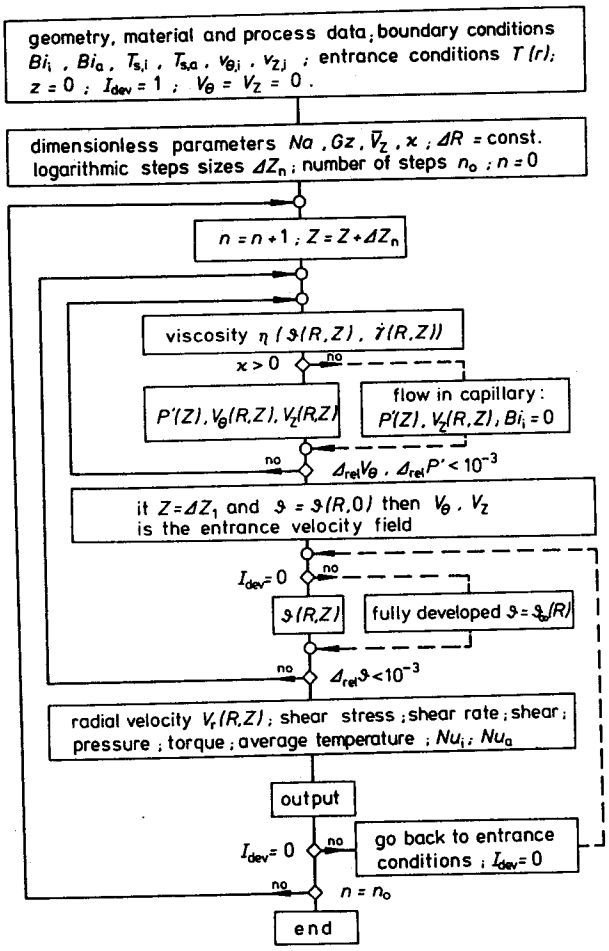

FIG. 7. Flow chart of universal shear flow program.

The axial velocity V_Z and the pressure gradient P' are calculated from the Z component of the equation of motion together with the integral of the flow rate (Eqs. (2.51) and (2.53)). The circular flow V_Θ is evaluated from the Θ component of the equation of motion (Eq. (2.50)). The R component V_R of the velocity supposedly does not influence the viscosity and the convection; thus it is calculated separately at the end of each step using the equation of continuity (a numerical method that allows for positive or negative radial flow contributions has been suggested by Gosman *et al.* [104]).

The entrance conditions are then stored, and the *fully developed temperature field* is calculated so as to be available as a reference state for the developing temperature field. In the fully developed temperature field, the convective term of the energy equation is zero. The iteration starts out with the viscosities and velocities at the entrance. They give a first approximation of the dissipation term and of the fully developed temperature field. Using this solution, one gets improved values of the viscosities and the velocities by iteration. These values of the viscosities and velocities lead to the second approximation of the fully developed temperature field, and so on. After satisfying the condition of $(\Delta_{rel}\vartheta < 10^{-3})$, the values of $(\vartheta_\infty - \vartheta(\kappa, \infty))$ and of $(\vartheta_\infty - \vartheta(1, \infty))$ are stored as reference values for the developing temperature field. Then the program goes back to the entrance temperature field and starts calculating the developing temperature, velocity, shear stress, and pressure. If both walls are adiabatic ($Bi_i = Bi_a = 0$), there does not exist a fully developed temperature field; the program then starts calculating the developing temperatures immediately.

For flow in a capillary ($\kappa = 0$), the velocity and the temperature have a zero gradient at $R = 0$.

The power law model fails in describing the viscosity at low shear rates, and for computational purposes at least one has to set an upper limiting value of the viscosity (this has been done in the numerical program of this study). For more accurate calculations, one has to approximate ranges of the viscosity curve by several power law and temperature coefficients. Also a viscosity table could be used instead.

The numerical program has been checked with analytical solutions of the fully developed temperature and velocity field in plane Couette flow and with isothermal flow in a pipe and in an annulus [105].

Besides helical flow with its steady, but developing temperature field, the system of equations, Eqs. (2.35)–(2.37), describes the flow geometries of all other steady shear flows with open stream lines (type a_1–h in Table V). Therefore, it actually is possible to *use one numerical program for all these flow cases.* The appropriate values of the ratio of the radii κ, the axial velocity of the inner cylinder $V_Z(\kappa, Z)$, and the average axial velocity $\bar{V}_Z$ are listed in Table VI.

TABLE VI

SHEAR FLOW GEOMETRIES AS LIMITING CASES OF HELICAL FLOW[a]

Flow geometry as described in Fig. 3	κ	$V_Z(\kappa, Z)$	$\bar{V}_Z$
a_1	0.999	2	1
b	$0 < \kappa < 1$	determined by iteration for $P' = 0$	1
c	0	—	1
d	0.999	0	1
e	$0 < \kappa < 1$	0	1
f	$0 < \kappa < 1$	0	$0 < \bar{V}_Z < 1$
g	$0 < \kappa < 1$	finite	1
h	0.999	finite	1
a_2	0.999	0	0
i	$0 < \kappa < 1$	0	0

[a] Listing of the corresponding geometry (described with κ) and kinematics (described with the velocity of the inner cylinder $V_Z(\kappa, Z)$ and the average axial velocity $\bar{V}_Z$). Geometries a_1–h are with open, and geometries a_2 and i with closed stream lines.

Due to the parabolical character of the solution procedure for the equation of energy, the helical flow program can be applied only to flows with non-negative velocity components. Thus, axial drag flow in an annulus with nonzero axial pressure gradient (type g) and drag flow in a narrow slit between two parallel plates with nonzero pressure gradient (type h) can be analyzed only up to moderate positive pressure gradients. A solution procedure that allows for back flow is described in the literature [104], but it does not seem to have been applied to these types of flow.

4. *Calculated Results*

There is a large variety of heat transfer problems solvable with the universal shear flow program. Some examples follow, mainly concerning the thermal boundary conditions (Biot number) and the kinematics for various shear flow geometries. Similar examples of helical flow or annular flow calculations have already been published, however, with idealized thermal boundary conditions [85]. In all the examples of this section, the entrance temperature (at $Z = 0$) is taken to be $\vartheta_e(R) = 0$.

The *thermal boundary conditions* influence the developing temperatures and velocities to a large extent. In analytical studies generally, idealized conditions are assumed, i.e., isothermal or adiabatical wall; in real flow